

# Divergent gametic thermal performance and floral warming across an elevation gradient

Jacob M. Heiling<sup>1,2, ID</sup> and Matthew H. Koski<sup>1, ID</sup>

<sup>1</sup>Department of Biological Sciences, Clemson University, Clemson, SC, United States

<sup>2</sup>Biology Department, Western Carolina University, Cullowhee, NC, United States

Corresponding author: Biology Department, Western Carolina University, Biology 1 University Dr, Apodaca Science Building, Cullowhee, North Carolina 28723, United States. Email: [jheiling@wcu.edu](mailto:jheiling@wcu.edu)

## Abstract

Thermal environments vary widely across species ranges, establishing the potential for local adaptation of thermal performance optima and tolerance. In the absence of local adaptation, selection should favor mechanisms to meet thermal optima. Floral temperature is a major determinant of reproductive success in angiosperms, yet whether gametic thermal performance shows signatures of local adaptation across temperature gradients, and how variation in gametic thermal performance influences floral evolution, is unknown. We characterized flowering season temperatures for the forb, *Argentina anserina*, at extremes of a 1000 m elevation gradient and generated thermal performance curves for pollen and ovule performance in populations at each extreme. Thermal optima fell between mean and maximum intrafloral temperatures. However, cooler high-elevation populations had ~4 °C greater pollen thermal optima than warmer low-elevation populations, while tolerance breadths did not differ. We then tested whether plants at elevational extremes differentially warmed the floral microenvironment. High-elevation flowers warmed significantly more than low, bringing intrafloral temperatures nearer the pollen optima. A manipulative experiment demonstrated that stronger warming in high elevation was conferred by floral tissues. Elevational divergence in floral warming may be driven, in part, by selection on flowers to meet different thermal demands of the gametophytes.

**Keywords:** *Argentina anserina*, floral evolution, gamete performance, local adaptation, thermal performance, thermoregulation

## Introduction

Temperature is perhaps the most universal abiotic factor affecting the presence, performance, and survival of organisms across the biosphere. The thermal environment varies dramatically in both time and space across species' distributions, especially those spanning wide latitudinal or elevational ranges (e.g., [Sunday et al., 2019](#)). Such variation in the thermal environment may result in local adaptation of thermal performance optima, and tolerance breadth (e.g., [Bennett et al., 2021](#); [Higgins et al., 2014](#)). This may present as the evolution of tolerance to temperature extremes ([Davies & Hew, 1990](#); [Griffith & Yaish, 2004](#); [Schlesinger, 1990](#)), temperature variability ([Gaston et al., 2009](#); [J. Sunday et al., 2019](#); [Janzen, 1967](#); [Pither, 2003](#); [Stevens, 1989](#)), or escape in time via evolved or plastic phenological shifts ([Rathcke & Lacey, 1985](#)). In the absence of local adaptation of thermal performance or phenological escape, organisms can employ a variety of metabolic ([Laloi et al., 1997](#); [Navas, 1997](#)), physiological ([Gates, 1968](#); [Seebacher & Franklin, 2005](#)), or behavioral ([Buckley et al., 2015](#); [Clench, 1966](#); [Heinrich & Esch, 1994](#); [Kingsolver, 1987](#)) mechanisms to reach optima and stay within tolerance zones.

There is abundant evidence of predictable variation in metrics of thermal tolerance ([Sunday et al., 2019](#)) and performance ([Porcelli et al., 2017](#); [Sunday et al., 2014](#)) across latitudinal and elevational gradients, reflecting responses to variable selection by the thermal environment. For instance,

warmer low-elevation populations often exhibit greater thermal optima than cooler high-elevation populations ([Gilbert & Miles, 2019](#)). Unsurprisingly, these patterns are often stronger for ectotherms than endotherms (e.g.: [Sunday et al., 2019](#)). For species with limited mobility or dispersal capacity, local adaptation to thermal conditions should be especially common.

As sessile ectotherms ([Lacey et al., 2010](#)), angiosperms should experience particularly strong selection on thermal tolerance, traits mediating plant temperature, or both. The thermal ecology of plant primary metabolism and growth is well-studied ([Geange et al., 2021](#); [Sage & Kubien, 2007](#); [Sheth & Angert, 2014](#); [Smith & Dukes, 2013](#); [Yamori et al., 2014](#)). More recently, focus has turned to the thermal ecology of sexual processes, encompassing gametophyte development, the progamic phase of mature gametophytes (anthesis to fertilization), and post-zygotic processes (zygote development and seed maturation) ([Flores-Rentería et al., 2018](#); [van der Kooi et al., 2019](#)). Of these, the progamic phase deserves special attention given the importance of anthesis and gametophyte dispersal to plant reproduction and the fact that pollen in transit is among the most thermally sensitive component of plant reproduction ([Chaturvedi et al., 2021](#)). While gametic thermal ecology in the progamic phase has received notable attention in recent years (e.g., [Rosbakh & Poschlod, 2016](#)) this still represents a gap in our knowledge of plant reproductive ecology as well as thermal ecology of ectotherms more

Received June 12, 2023; revisions received December 13, 2023; accepted December 29, 2023

Associate Editor: Jannice Friedman; Handling Editor: Tim Connallon

© The Author(s) 2023. Published by Oxford University Press on behalf of The Society for the Study of Evolution (SSE).

This is an Open Access article distributed under the terms of the Creative Commons Attribution-NonCommercial License (<https://creativecommons.org/licenses/by-nc/4.0/>), which permits non-commercial re-use, distribution, and reproduction in any medium, provided the original work is properly cited. For commercial re-use, please contact [journals.permissions@oup.com](mailto:journals.permissions@oup.com)

broadly (Leith et al., 2022), particularly external fertilizers (Chirgwin et al., 2021).

During the progamic phase, the gametophyte-bearing structures within flowers (anthers and gynoecium) are exposed to the external environment, rendering flowering among the life stages most sensitive to temperature (Hatfield & Prueger, 2015; Zinn et al., 2010). Reproductive success can be limited during the flowering stage not only by temperature extremes (Gezon et al., 2016; Giorno et al., 2013) but also by deviations in mean temperatures from performance optima (Lacey et al., 2010; Mareri & Cai, 2022; Rosbakh et al., 2018). Direct effects of the thermal environment on plant reproductive success should impose selection on the position of thermal optima and tolerance breadth. In addition to direct selection on gamete optima and tolerance, traits that modify the intrafloral temperature in which gametes operate may also be targets of selection. Flowers exhibit a variety of potential mechanisms that may help to buffer the effects of the external thermal environment on sensitive floral tissues and gametes (van der Kooi et al., 2019).

Floral thermoregulatory mechanisms should be subject to selection when environmental temperatures are not optimal for gamete performance or exceed their tolerance breadth. Mechanisms that promote heat accumulation in flowers, such as heliotropism or parabolic petal arrangement are common (e.g., Corbett et al., 1992; Creux et al., 2021; Galen & Stanton, 2003; Harrap et al., 2017; Kevan, 1972). Intrafloral heat accumulation can confer fitness advantages for pollen and ovules (Corbett et al., 1992; Galen & Stanton, 2003), and pollinator attraction (Creux et al., 2021). Flowers can also limit heat accumulation by altering the orientation of petals (van der Kooi et al., 2019) or through evaporative cooling (Patiño & Grace, 2002). These mechanisms may function to bring intrafloral temperatures closer to gametic thermal optima under suboptimal ambient thermal conditions.

For angiosperms spanning wide latitudinal or elevational ranges, temperature means and extremes during flowering often differ substantially among populations (e.g., Flores-Rentería et al., 2018; Lacey et al., 2010). Thus, directional

selection on gametic thermal performance may lead to clinal variation among populations in thermal optima, tolerance breadths, and/or floral warming/cooling (Figure 1A–C). First, if the thermal environment selects on performance optima directly, then optima should closely align with environmental temperatures (Figure 1A). Second, selection may act to expand thermal tolerance breadths such that they better coincide with the ambient temperature range along the gradient (Figure 1B). This could take the form of increased tolerance breadth when thermal optima deviate further from environmental temperature (e.g., wider shaded area in Figure 1B), asymmetric tolerance breadths biased in the direction of the environmental mean (e.g., asymmetric shaded bars, Figure 1B), or both. Finally, selection may favor warming or cooling mechanisms that facilitate favorable intrafloral temperatures despite unfavorable external temperatures (Figure 1C). Selection favoring these mechanisms should be strongest when gametic thermal optima deviate dramatically from environmental temperatures. None of these responses are mutually exclusive and differentiation among populations can indicate whether a given evolutionary response has occurred.

Here we used the cosmopolitan forb *Argentina anserina* (“silverweed”) (Rosaceae) to evaluate gametic thermal performance metrics at the elevational extremes of a 1000 m elevation gradient in southwestern Colorado, USA. We used a combination of long-term ambient temperature data and direct field measurements of intrafloral and flower-level ambient temperatures (the temperature within the corolla and the ambient temperature at flower height) to compare the floral thermal environment between low- and high-elevation extremes. We generated thermal performance curves for three key post-pollination processes (pollen germination, pollen tube growth, and seed initiation) in low- and high-elevation populations. Finally, we performed a field experiment to determine the degree to which floral warming or cooling could be attributed to effects of the perianth (petals and sepals).

We leveraged these datasets to address four questions. First, we asked: are the relationships between local temperatures and (1) gametic thermal optima and (2) tolerance breadths

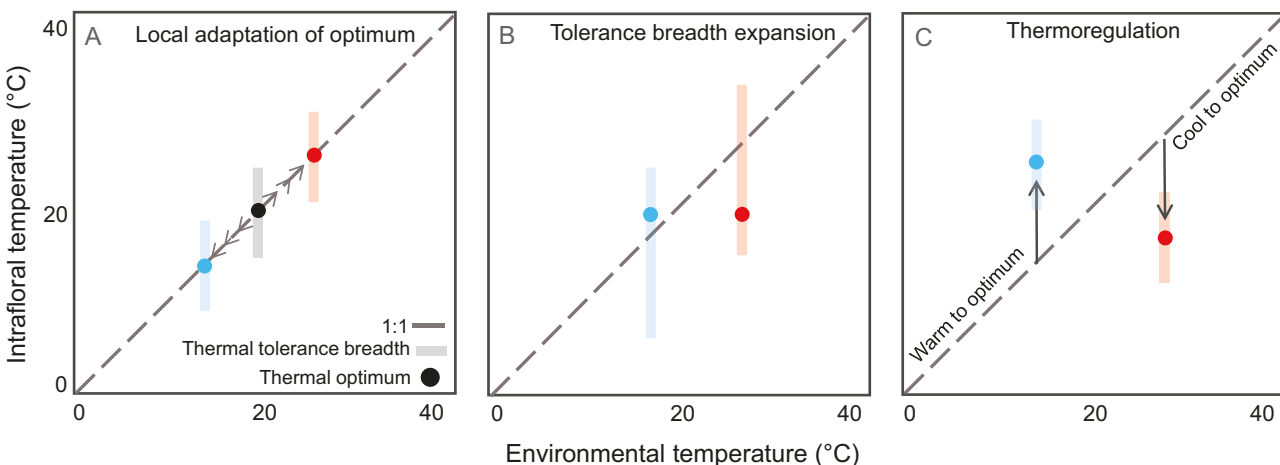


**Figure 1.** Three potential responses to non-optimal thermal environments for sessile ectotherms. We discuss these in the context of gametic thermal performance, but they may be generalized to any thermal performance metric. Position on the X-axis represents mean temperature (°C) during gamete dispersal/fertilization in a given environment, and position on Y-axis represents gametic performance optimum. Panel A represents an evolutionary response of the thermal performance optima to local temperature. Panel B represents an evolutionary response of thermal tolerance breadth. Panel C represents an evolutionary response of warming or cooling mechanisms to meet the demands of the thermal environment when the thermal optima or breadths are not locally adapted.

consistent with local adaptation to thermal environment? Finding that ambient temperatures often fell short of gametic optima, especially in cooler high-elevation populations, we asked (3) whether intrafloral heat accumulation helped to compensate for differences between the ambient temperature and the gametic optima, whether this varied with elevation, and (4) whether perianth tissue explained differences in floral warming between low- and high-elevation populations.

## Methods

### Study system

*Argentina anserina* (L.) Rydb. (syn. *Potentilla anserina*; Rosaceae) is a cosmopolitan species aggregate of stoloniferous forbs common to wet meadows and margins of water-bodies (Rousi, 1965). In North America, it occurs from sea level to ca. 3,500 m.a.s.l (Rousi, 1965). Here, we focus on *A. anserina* in southwestern Colorado, where populations occur from the montane to subalpine zones (Weber & Wittman, 1996), with peak flowering occurring from June to July. Low- and high-elevation populations flower simultaneously (Koski et al., 2022). Flowers are small (1–2 cm diam.) five-petaled hypanthium borne signally from the basal rosette or stolon nodes 0.5–20 cm above the soil surface. The hermaphroditic flowers are largely self-incompatible (Cisternas-Fuentes et al., 2022) and are pollinated by flies and small bees (Koski & Ashman, 2015). Anthesis lasts ~48 hr and there is no evidence of dichogamy (Cisternas-Fuentes et al., 2022). Petals open in the morning and anthers dehisce the first day. Petals close over reproductive structures in the evening on the first day and then reopen on the second day. All plant material used for growth chamber experiments in this study was cloned from field-collected plants from six populations occurring from approx. 2,300 to 3,400 m.a.s.l (Table 1) in the San Juan Mountains.

### Long-term thermal environments of *A. anserina* populations

We used the Oregon State University PRISM database to extract long-term monthly minima, maxima, and mean temperatures (hereafter, “ambient”) for six low (<3,000 m.a.s.l) and four high- (>3,000 m.a.s.l) elevation *A. anserina* populations in SW Colorado for June and July (peak flowering period) from 1969 to 2020 at a 4-km resolution (PRISM Climate Group, Oregon State University, <https://prism.oregonstate.edu>, data accessed September 1, 2021). This dataset (hereafter, long-term ambient) describes the thermal environment recorded approx. 2 m above the soil surface.

### Intrafloral and flower-level ambient temperature in the field

We directly measured the intrafloral and flower-level ambient temperatures in five low-elevation (2,347–2,613 m.a.s.l, Table 1) and four high-elevation populations (3,113–3,435 m.a.s.l, Table 1) using K-type thermocouples placed within (intrafloral), and directly adjacent to flowers (flower-level ambient, ~2 cm from flower) in June–July 2021. We selected flowers on the first day of anthesis. As flowers opened in the morning, we taped intrafloral probes to the pedicel and bent them into the floral disk. This allowed petals to open and close without disturbing the thermocouple. Each ambient thermocouple was fastened to a dowel at flower level with the probe suspended in the air. Thermocouples were connected to Omega dataloggers

**Table 1.** Temperature differences between low- (<3,000 m) and high- (>3,000 m) elevation populations of *Argentina anserina* using long-term daily mean ambient temperature during peak flowering (June–July), ambient temperature at flower-level 24 hr intrafloral temperature, and daytime intrafloral temperature. Bottom row: Wilcoxon rank sum tests comparing low versus high population minima, means, and maxima. Statistical tests in bold are significant at  $\alpha < 0.05$ . Genotypes from populations in bold were used to generate thermal performance curves for this study.

Elevation group	Population	Elevation (m.a.s.l)	Long-term (1969–2020)			Flower-level ambient (2021)			24 hr Intrafloral (2021)			10:00–18:00 Intrafloral (2021)		
			Min	Mean	Max	Min	Mean	Max	Min	Mean	Max	Min	Mean	Max
Low	MWL	2347	4.58	15.10	25.63	—	—	—	—	—	—	—	—	—
	M93	2414	0.40	15.08	29.80	0.17	14.49	39.37	0.69	14.34	36.52	15.73	23.89	35.20
	GVY	2459	1.20	15.25	29.80	3.50	15.27	42.37	3.60	15.36	37.48	15.75	24.53	35.22
	LJY	2534	0.60	15.33	30.30	2.67	15.63	42.53	4.88	15.14	35.79	14.04	23.50	34.21
	BL	2564	5.77	15.32	24.87	4.50	15.32	35.80	4.24	15.51	35.95	14.36	24.25	35.16
	BU	2613				1.70	14.69	37.34	4.17	16.48	36.70	17.05	25.01	34.94
Overall		2.51	15.22	28.08	2.51	15.08	39.48	3.51	15.37	36.49	15.39	24.23	34.95	
High	TCT	3113	2.54	11.19	19.84	-0.42	11.56	39.30	0.92	12.57	36.36	14.02	22.21	33.79
	CD	3289	-2.2	10.45	23.70	-0.225	10.69	34.03	2.11	11.86	33.38	12.09	19.45	28.76
	RL	3420	2.87	10.31	17.76	0.98	13.96	39.83	1.78	13.95	34.95	16.41	24.00	33.78
	FR	3435				1.63	13.96	32.85	2.56	13.87	33.04	17.96	24.28	32.73
Overall		1.07	10.65	20.43	1.31	12.54	36.50	1.84	13.06	34.43	15.12	22.49	32.27	
Wilcoxon rank sum		<b>P = 0.79</b>	<b>P = 0.035</b>	<b>P = 0.063</b>	<b>P = 0.019</b>	<b>P = 0.29</b>	<b>P = 0.19</b>	<b>P = 0.016</b>	<b>P = 0.91</b>	<b>P = 0.063</b>	<b>P = 0.91</b>	<b>P = 0.29</b>	<b>P = 0.016</b>	<b>W = 20</b>
		<b>W = 9</b>	<b>W = 15</b>	<b>W = 15</b>	<b>W = 18</b>	<b>W = 15</b>	<b>W = 15</b>	<b>W = 16</b>	<b>W = 18</b>	<b>W = 18</b>	<b>W = 15</b>	<b>W = 15</b>	<b>W = 20</b>	

(Omega Engineering Inc., Norwalk, CT, USA) which recorded temperature for 24 hr at 1-min intervals. Pairing intrafloral and ambient temperature data allowed us to calculate  $\Delta T$ , the difference between the intrafloral and ambient temperature, for each focal flower.  $\Delta T$  measures the degree to which floral interiors are above ( $\Delta T > 0$ ) or below ( $\Delta T < 0$ ) ambient temperatures. We sampled sites a mean of four times throughout peak flowering with at least two loggers (~6 intrafloral probes per logger; [Supplementary Table S1](#)). One low-elevation site, BL, was only sampled once due to sheep disturbance. Overall, we measured intrafloral and ambient temperature of 174 flowers across four high-elevation populations, and 135 flowers across five low-elevation populations.

We calculated  $\Delta T$  for each flower for each minute of logging, and grouped measurements into one of six 4 hr time bins (6:01–10:00; 10:01–14:00, 14:01–18:00; 18:01–22:00, 22:01–2:00, 2:01–6:00). Time bins were selected to capture distinct periods associated with floral anthesis and closure, pollen presentation, solar exposure, and pollinator activity. The 6:01–10:00 time bin captures floral anthesis and anther dehiscence, the onset of pollinator activity, and increasing solar irradiance. Whereas the 10:01–14:00 time bin captures peak pollinator activity and peak solar irradiance, and 14:01–18:00 captures declining pollinator activity and a reduction in solar irradiance. 18:01–22:00 captures the closure of petals and sunset, while the final two time blocks capture the coolest night-time temperatures. We used these data to test whether  $\Delta T$  differed between low and high elevation and to identify diel patterns in  $\Delta T$ .

### Plant material for thermal performance curves

In Summer 2019, 20–30 plants from three low- and three high-elevation populations were collected from the field ([Table 1](#)). Within each population, we collected plants every 2 + m to avoid re-sampling genets. Plants were kept as stock populations in a greenhouse in Clemson, SC in a 3:1 (v:v) mix of Fafard (Sungro Horticulture, Agawan, MA, USA) and Turface (Profile Products, Buffalo Grove, Ill, USA). In the fall of 2020, we cloned 20 maternal plants per population each eight times by stolon layering in separate pots. Clones were overwintered in a cold chamber at ~ 5 °C for 1.5 months before returning to the greenhouse in January 2021. The greenhouse was set to 19/15.5 °C (day/night) with a 12-hr day length. Peak flowering occurred from April to May. Daily mean greenhouse temperatures ranged between 13.8 and 20.6 °C during flowering but did not change directionally over time (temperature =  $-0.014$  (date) + 17.9,  $R^2 = 0.013$ ,  $p = .44$ ; [Supplementary Figure S1](#)). Thus, flowering time of a given individual in the greenhouse was decoupled from the temperature it was exposed to during floral development.

### Temperature treatments for thermal performance curves

We established seven temperature treatments spanning 0–39 °C ([Table 2](#)) to evaluate gametic thermal performance in growth chambers. These fall within the temperature range expected across low- and high-elevation sites in June–July based on the long-term ambient temperature ([Table 1](#)). The temperature treatment range was more conservative than extremes in the field ([Table 1](#)) due to the limits of the AL-41L4 Percival chambers (Percival Scientific, Perry, Iowa, USA). Relative humidity (%RH) setpoints were 32% and 50% day/night. These values were derived from mean day/night %RH

**Table 2.** Day and night temperature treatments. All treatments ran for 48 hr under a 14:10-hr day:night cycle. Relative humidity (RH) setpoints were 32 and 50 for day and night, respectively, for all treatments. RH setpoints were derived from mean day/night %RH for Denver, Grand Junction, and Colorado Springs in July ([NOAA, 2018](#)). Light intensity (full) constant across treatments.

Treatment	Temperature (°C)	
	Day	Night
T1	3	0
T2	9	6
T3	15	12
T4	21	18
T5	27	24
T6	33	30
T7	39	36

for Denver, Grand Junction, and Colorado Springs in July ([NOAA, 2018](#)).

Upon initiation of flowering in the greenhouse (March 2021), clones of each genotype were selected at random and moved to one of the seven temperature treatments. Two treatments were run simultaneously for 48 hr in separate chambers on a randomized schedule. To expose one clone per genotype to each temperature treatment, all temperature regimes were run at least twice. A given temperature treatment was alternated between the two chambers such that treatment and chamber identity were not confounded. A minimum of seven genotypes per population (range: 7–17; mean: 11; [Supplementary Table S2](#)) were exposed to each temperature treatment over the course of two to five runs per treatment to assess pollen and ovule viability.

### Flower preparation for gametic thermal performance curves

To isolate the effects of growth chamber temperatures on gamete performance, we removed corolla and calyx tissue to prevent potential warming or cooling of the gynoecia and androecia. That is, we wanted the floral microenvironment to experience temperatures as close as possible to the set temperature treatments by minimizing the potential for floral thermoregulation. Accordingly, we used dissecting scissors to remove petals and sepals from all experimental flowers prior to placement in growth chambers. We emasculated flowers destined for ovule performance assessment (one per clone) to prevent self-pollen from interfering with germination of outcross pollen following subsequent hand pollination. Experimental flowers were always chosen on the first day of anthesis and marked with jeweler's tags for identification.

### Pollen performance

After 24 hr of exposure to temperature treatment, we collected anthers from flowers assigned to pollen performance assessment and sonicated pollen into 0.2 ml vials containing 100  $\mu$ l of 10% sucrose (v/v) Brewbaker–Kwack (BK) solution ([Kearns & Inouye, 1993](#)). Vials were returned to the growth chambers where pollen germinated for 24 hr in the assigned treatment. We removed vials from growth chambers at the end of the second 24-hr period and pipetted 5  $\mu$ l of Farmer's fixative (3:1 v/v 95% ETOH and glacial acetic acid; [Kearns & Inouye, 1993](#)) into each vial to arrest germination and

tube elongation. We then mounted 10  $\mu$ l of solution on glass slides with glass coverslips, sealing each mount with clear nail varnish.

To quantify pollen performance, we scored pollen germination proportion and mean pollen tube length. To score pollen germination rate, we counted the number of grains out of 300 with pollen tubes longer than the diameter of the grain. To estimate pollen tube length, we photographed three fields on each pollen slide at 100  $\times$  magnification and measured the length of tubes in each image with the freehand line selection tool in ImageJ (Schneider et al., 2012). We then calculated mean tube length for each set of pooled images across a given sample. In total, we scored germination rate and tube length on 559 samples and 312 samples, respectively.

### Ovule performance

After 24 hr of exposure, we hand-pollinated each flower assigned to the ovule performance assessment group. We used a camel hair brush to apply pollen (Kearns & Inouye, 1993) collected from 3 to 5 donors from the same population from a pool of pollen-donor plants kept in the greenhouse. Following hand pollination, plants were maintained in growth chambers for 24 hr to allow fertilization to occur in the assigned temperature treatment, after which plants were returned to the greenhouse. Thus, maternal plants were pollinated and fertilized under treatment conditions, while pollen donors were kept at an intermediate temperature. By allowing seeds to develop in greenhouse conditions post-fertilization rather than under their respective temperature treatments, we isolated the effects of the thermal environment on the progamic phase (pollination through fertilization) of ovule performance from subsequent post-zygotic processes occurring from fertilization through seed maturation. Fruits were allowed to develop until ripe (~April–May 2021), at which point they were removed from plants and stored in coin envelopes to dry prior to seed counting.

To quantify ovule performance, we calculated seed set as the proportion of mature seeds produced by each fruit to mean ovule number for each population rounded to the nearest integer. Population mean ovule number was generated by counting ovules in 11–42 field-collected flowers per population (mean across populations = 27.75, range of population means = 23.17–30.91). Specifically, fresh flowers were collected in the field in 70% EtOH, and returned to the lab to be counted under a dissecting microscope. In total, we scored seed set for 495 fruits. Seed set could exceed 1 when seed number was greater than mean population ovule number (6.6% of fruits).

### The effect of the perianth on intrafloral temperature

To assess the effect of the perianth on intrafloral temperature in the field, we experimentally cut petal and sepal tissue from flowers and measured intrafloral and flower-level ambient temperature in a subset of low- and high-elevation populations. Each cut flower was paired with a control flower on the same individual for which we left petal and sepal tissue intact. We measured temperature for 24 hr at 1-min intervals for 16 pairs in low-elevation sites and 50 pairs in high-elevation sites. We calculated  $\Delta T$  for each minute of logging and grouped them into six 4-hr time bins as above.

### Statistics

All analyses were performed in R (R Core Team, 2021). Thermal performance curves were constructed using

R version 3.6.3. All other analyses were performed using R version 4.2.2.

### Elevational differences in the thermal environment

We used Wilcoxon rank sum tests (R *stats* package) to compare monthly long-term ambient temperature minima, means, maxima, and ranges between the high- ( $n = 4$ ) and low- ( $n = 6$ ) elevation sites, as reported by PRISM for peak flowering of *A. anserina* in our focal region, June and July (pooled) 1969–2020. We chose the Wilcoxon test because data were not normally distributed.

We compared flower-level ambient and intrafloral temperature minima, means, maxima, and ranges between the high- ( $n = 4$ ) and low- ( $n = 5$ ) elevation sites using Wilcoxon rank sum tests. We also assessed whether long-term ambient and flower-level ambient thermal environments were similar, using Welch's two-sample *t*-tests to compare each long-term ambient metric and the corresponding flower-level ambient metric within each elevation group. Comparisons of flower-level ambient and intrafloral temperatures are described under *Flower warming and cooling* below.

### Thermal performance curves

We generated thermal performance curves (hereafter, TPCs) for pollen germination, pollen tube length, and seed set to estimate optimal performance temperature ( $T_{opt}$ ) and 50% tolerance breadth ( $B_{50}$ ) for each of the six focal populations separately. Specifically, we used the *minpack.lm* package in R (Elzhov et al., 2016) to model each performance metric as a function of temperature using Gaussian, quadratic, and Kumaraswamy functions using *nlsLM* (e.g., Angilletta, 2006; Clay & Gifford, 2017; Kingsolver & Woods, 2016; Palaima & Spitze, 2004; Sheth & Angert, 2014; code provided by S. Sheth). We additionally generated a TPC using a beta distribution (Clay & Gifford, 2017) for pollen germination because it was bound between 0 and 1. We could not generate a TPC for seed set in one population (MWL, Supplementary Table S1) because no seeds were produced following hand pollinations. We compared model AICs to determine the best-fit model for each population and performance metric.

For pollen tube length, the Gaussian distribution provided the best fit in each population (Supplementary Table S3). For seed set, the Gaussian provided the best fit in all but one population for which the quadratic fit modestly better (population BL, Supplementary Table S3). However, for standardized comparisons among populations, we present the Gaussian fit for seed set in this population. For pollen germination, the Gaussian distribution provided the best fit for half of the populations (all at least three AIC points lower than the beta distribution; Supplementary Table S3), while the beta distribution modestly outperformed the Gaussian in the other half (all less than 1 AIC point lower than Gaussian; Supplementary Table S3). Performance optima from a Gaussian and beta distribution were tightly correlated for pollen germination ( $r = 0.98$ ,  $p < .001$ ,  $N = 6$ ; Supplementary Table S4). Thus, analyzing TPC metrics generated from a Gaussian and a beta distribution yielded similar results. Because the Gaussian was best fit overall across populations, we present Gaussian TPCs. Parameters from TPCs for pollen germination fit with the beta distribution in all populations are provided in Supplementary Table S4 and plots of curves are provided in Supplementary Figure S3.

From TPCs, we extracted the maximum performance, the temperature at peak performance ( $T_{opt}$ ), and the temperature

breadth at 50% of the maximum performance value ( $B_{50}$ ; Huey & Stevenson, 1979; Sheth & Angert, 2014; Sinclair et al., 2016). We used Welch's two-sample *t*-tests to compare high- and low-elevation  $T_{opt}$  and  $B_{50}$  for each gamete performance metric. Because TPCs for pollen germination produced using the beta distribution generated tolerance breadths that were asymmetrically skewed left in each population (Supplementary Figures S3 and S4), we also calculated the degree of asymmetry in breadth around the optimum as  $[(T_{opt} - T_{low50})/(B_{50})]$  where  $T_{low50}$  is the lower temperature at which the TPC is at 50% of peak performance. We compared the skew metric between low- and high-elevation populations using Welch's two-sample *t*-test.

### Thermal performance in relation to environmental temperatures

We performed one-way Z-tests to assess whether the thermal optima for each reproductive metric (pollen germination, pollen tube elongation, and seed set) differed from the thermal environment. We used the long-term ambient and the intrafloral temperature datasets to capture the broadest possible scope of the thermal environment that our data allow. For both temperature datasets, we compared thermal optima to the minimum, mean, and maximum environmental temperatures. For the long-term ambient temperature dataset, we calculated temperature minimums, means, and maximums using population-level monthly means. For the intrafloral temperature dataset, we used individual-level mean temperatures pooled across populations as replicates for analysis at the elevation-group level. We analyzed the intrafloral temperature dataset at two time scales: the full 24-hr sampling period, and an 8-hr subset ("daytime," 10:01–18:00). This daytime scale represents the intrafloral microenvironment during exposure to direct sun.

To evaluate whether thermal tolerance breadth was larger when the thermal optima deviated further from the ambient thermal environment (Figure 1B), we measured Pearson correlations between  $B_{50}$  and the absolute value of the differences between the gametic thermal optima and the mean flower-level and long-term ambient temperatures (from here: "optima-distance") for each site. Here, we did not use the intrafloral dataset because intrafloral temperatures may systematically differ from the ambient conditions (see *Flower warming and cooling*). For this analysis, each population served as a replicate. A positive correlation would correspond to  $B_{50}$  increasing as environmental temperatures diverge from the optima (consistent with the proposed pattern in Figure 1B in which selection widens tolerance breadths as the environment diverges from the optimum). We additionally correlated the degree of tolerance breadth asymmetry for pollen germination TPCs generated using the beta distribution with the optima-distance temperature metrics. Finally, we used Welch's two-sample *t*-tests to compare flower-level ambient and intrafloral temperatures during the peak of floral warming (T2, 10:01–14:00; T3, 14:01–18:00) to gametic thermal optima within each elevation group.

### Flower warming and cooling

Upon finding that pollen optima exceeded mean ambient temperatures, especially for high-elevation populations, we assessed whether low- and high-elevation populations differentially warmed the floral microenvironment. We modeled  $\Delta T$  at the flower level as a function of elevation (low vs. high),

time bin, and their interaction with population nested in elevation as a fixed term. We included flower identity nested in population as a random term to account for repeated measurements on individual flowers. We used type III SS for inference testing, and generated estimated marginal means for elevation class and time bin using the "emmeans" function. Because of a significant elevation  $\times$  time bin interaction, we tested whether  $\Delta T$  differed between elevation classes within each time bin using post hoc Tukey tests.

### Effect of the perianth on intrafloral temperature

We compared  $\Delta T$  between intact flowers and those with perianth tissue removed using a mixed-effect linear model using the lmer function in the R package *lme4* (Bates et al., 2015). We modeled  $\Delta T$  as a function of flower type (cut vs. intact), elevation class, time bin (10:01–14:00 and 14:01–18:00), and their interactions with population nested in elevation class as a fixed effect. To prevent pseudoreplication, we included flower identity nested within population, and sampling day nested in site as random terms. We used sampling day nested in site as a random term in the model to pair cut and intact flowers sampled in a given population on a given day. We generated estimated marginal means of each flower type within each elevation class and compared cut vs. intact flowers within time bin and elevation using post hoc Tukey tests using the emmeans function in the *emmeans* package (Lenth, 2022).

## Results

### Long-term thermal environment

Long-term ambient mean and maximum temperatures during peak flowering were 4.57 and 7.65 °C warmer in low-elevation populations than high, respectively (mean,  $W = 15$ ,  $p = .035$ ; maximum  $W = 15$ ,  $p = .036$ ; Table 1 and Figure 2). Low elevations were subject to a 6.21 °C broader temperature range than high, but this difference was not statistically significant ( $W = 13$ ,  $p = .143$ ; Table 1).

### Flower-level and intrafloral temperature

Overall, differences in mean flower-level ambient and intrafloral temperature minima, means, and maxima between low and high elevation in 2021 (Table 1C) reflected long-term temperature data (Table 1), with high-elevation flowers experiencing cooler temperatures and a narrower range than low. However, elevational differences were less pronounced than in the long-term ambient data. Mean temperatures differed between low and high elevation in both flower-level ambient and 24-hr intrafloral datasets, with low elevations experiencing 2.54 °C warmer mean flower-level ambient and 2.3 °C warmer intrafloral temperatures than high ( $W = 20$ ,  $p = .019$  and  $W = 20$ ,  $p = .016$ , respectively; Table 1C). Daytime intrafloral maxima differed most between low and high elevations (34.95 vs. 32.27 °C, respectively;  $W = 20$ ,  $p = .016$ ; Table 1). Flower-level ambient temperature maxima in 2021 were significantly warmer than long-term ambient maxima at ~2 m above the soil surface in both low- (39.48/28.08 °C) and high- (36.5/20.43 °C) elevation groups (low:  $T_{7.85} = -6.43$ ,  $p = .0002$ ; high:  $T_{4.85} = -6.44$ ,  $p = .0015$ ). Overall, intrafloral temperatures closely tracked flower-level ambient temperatures (Table 1), though notable differences are reported in floral warming and cooling ( $\Delta T$  analysis).

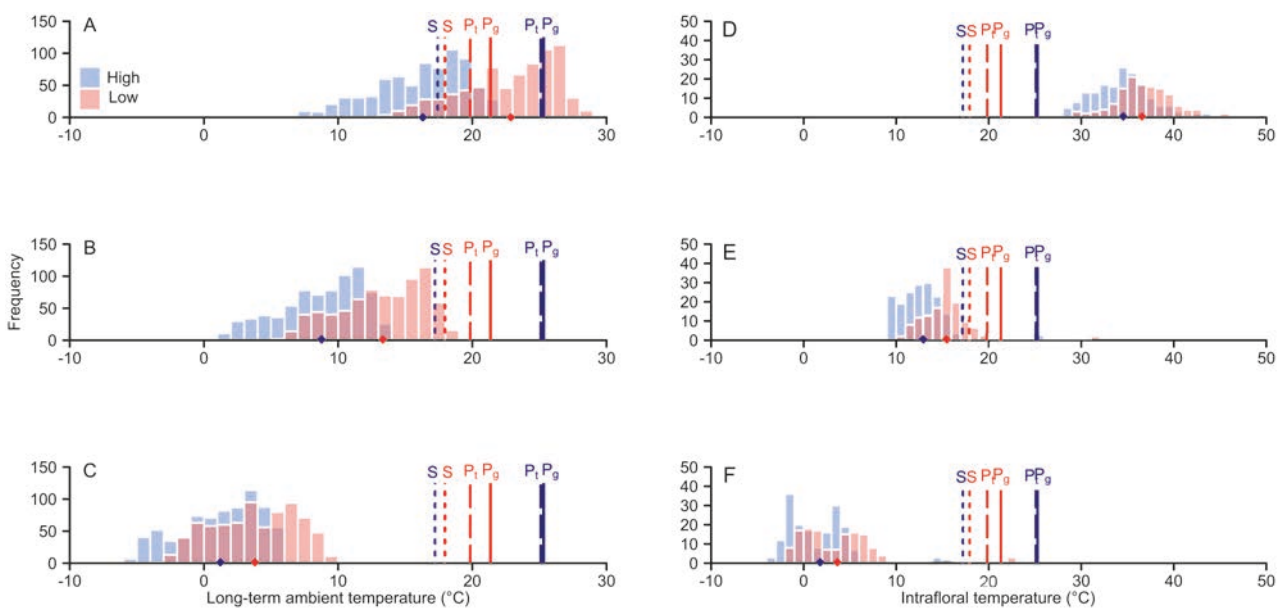


**Figure 2.** Histograms of mean long-term ambient, and field-measured intrafloral temperature maxima (A and D), means (B and E), and minima (C and F) for low- and high-elevation populations of *Argentina anserina*. For long-term ambient data, temperatures were recorded during the flowering season (June–July) from 1969 to 2020. For intrafloral data, temperature was recorded within flowers in June–July 2021. Vertical lines indicate  $T_{\text{opt}}$  of pollen germination ( $P_g$ ), pollen tube growth ( $P$ ), and seed set ( $S$ ). Diamonds represent high- and low-elevation mean thermal maxima (A and D), means (B and D), and minima (C and D) pooled across sites. All  $T_{\text{opt}}$  were significantly different from the means of the respective temperature distributions at  $\alpha = 0.05$ , as determined by one-sample Z-tests (Table 3).

## Thermal performance curves

### Performance optima

Pollen performance was strongly inhibited by extreme temperatures in both low- and high-elevation populations (Figure 3). Thermal optima for pollen germination ranged 19.5–22.7 °C among low-elevation populations while  $T_{\text{opt}}$  for tube length ranged 19.0–20.5 °C. Surprisingly,  $T_{\text{opt}}$  for both metrics of pollen performance were greater in high-elevation populations than low, ranging 24.2–27 °C, and 21.3–27.7 °C for germination and tube length, respectively. Mean  $T_{\text{opt}}$  of pollen germination was significantly warmer in high ( $\mu_{\text{high}} = 25.31$  °C) than in low ( $\mu_{\text{low}} = 21.35$  °C) populations ( $T_{3.97} = -3.11$ ;  $p = .036$ ). Likewise, optima for pollen tube length were also warmer in high- ( $\mu_{\text{high}} = 25.09$  °C) than in low- ( $\mu_{\text{low}} = 19.86$  °C) elevation populations, but this difference was not statistically significant ( $T_{2.21} = -2.66$ ;  $p = .106$ ).

Ovule performance (seed set) was far less responsive to temperature than pollen performance (Figure 3). However, in four of the five populations for which we generated TPCs, a significant  $T_{\text{opt}}$  for seed set was recovered (Supplementary Table S4).  $T_{\text{opt}}$  for seed set was similar ( $T_{1.36} = 0.69$ ;  $p = .59$ ) between high- ( $\mu_{\text{high}} = 19.86$  °C) and low- ( $\mu_{\text{low}} = 17.99$  °C) elevation populations (Figures 3 and 4).

### Tolerance breadth

The  $B_{50}$  for pollen germination was similar between low- and high-elevation populations (high: 17–26.1 °C, low: 15–23 °C; Figures 3 and 4).  $B_{50}$  for pollen tube length tended to be wider than for germination, but was similar between low- and high-elevation populations (high: 27.2–36.4 °C, low: 19.8–30.9 °C; Figures 3 and 4). Neither metric differed significantly between elevations. Asymmetry for  $B_{50}$  around the thermal optimum for pollen germination was detected when TPCs were generated with a beta distribution, with breadth being skewed toward cooler temperatures in all

populations. The degree of left-skew tended to be higher in high-elevation populations than low ( $\text{skew}_{\text{high}} = 0.576$ ,  $\text{skew}_{\text{low}} = 0.530$ ,  $t = 2.48$ ,  $p = .067$ ) though overall  $B_{50}$  did not differ ( $t = -1.55$ ,  $p = .196$ ).

$B_{50}$  for seed set could only be reliably obtained for populations in which the Gaussian TPC's standard deviation parameter was significantly different from zero. This was only the case in low-elevation populations (Supplementary Table S4), indicating that seed set in high-elevation populations was not impacted by extreme temperatures. For the low elevation populations that set seed, BL, and BU,  $B_{50}$  was 35.3 and 34.7 °C, respectively (Figure 3).

### Thermal performance in relation to environmental temperatures

#### Performance optima

Thermal optima for reproductive metrics were universally warmer than long-term ambient temperature minima and means for both high and low elevation (Table 3; Figure 2B and C). Low-elevation pollen and ovule optima were below long-term ambient maximum temperatures (Table 3, Figure 2A). However, pollen and ovule performance optima exceeded long-term ambient maxima at high-elevation sites (Table 3; Figure 2A).

At a 24-hr timescale, intrafloral minima and mean temperatures fell significantly below thermal optima for both pollen and ovule performance metrics for both elevation groups (Table 1, Figure 2E and F), while intrafloral maxima universally exceeded gametic thermal optima for both elevation groups (Table 1; Figure 2D). Patterns of daytime (10–18:00) intrafloral temperatures were qualitatively similar to the 24-hr scale, with two notable exceptions: daytime means exceeded (1) all gametic performance optima at low elevations (2) the ovule performance optimum at high elevations (Table 1; Figure 2E).

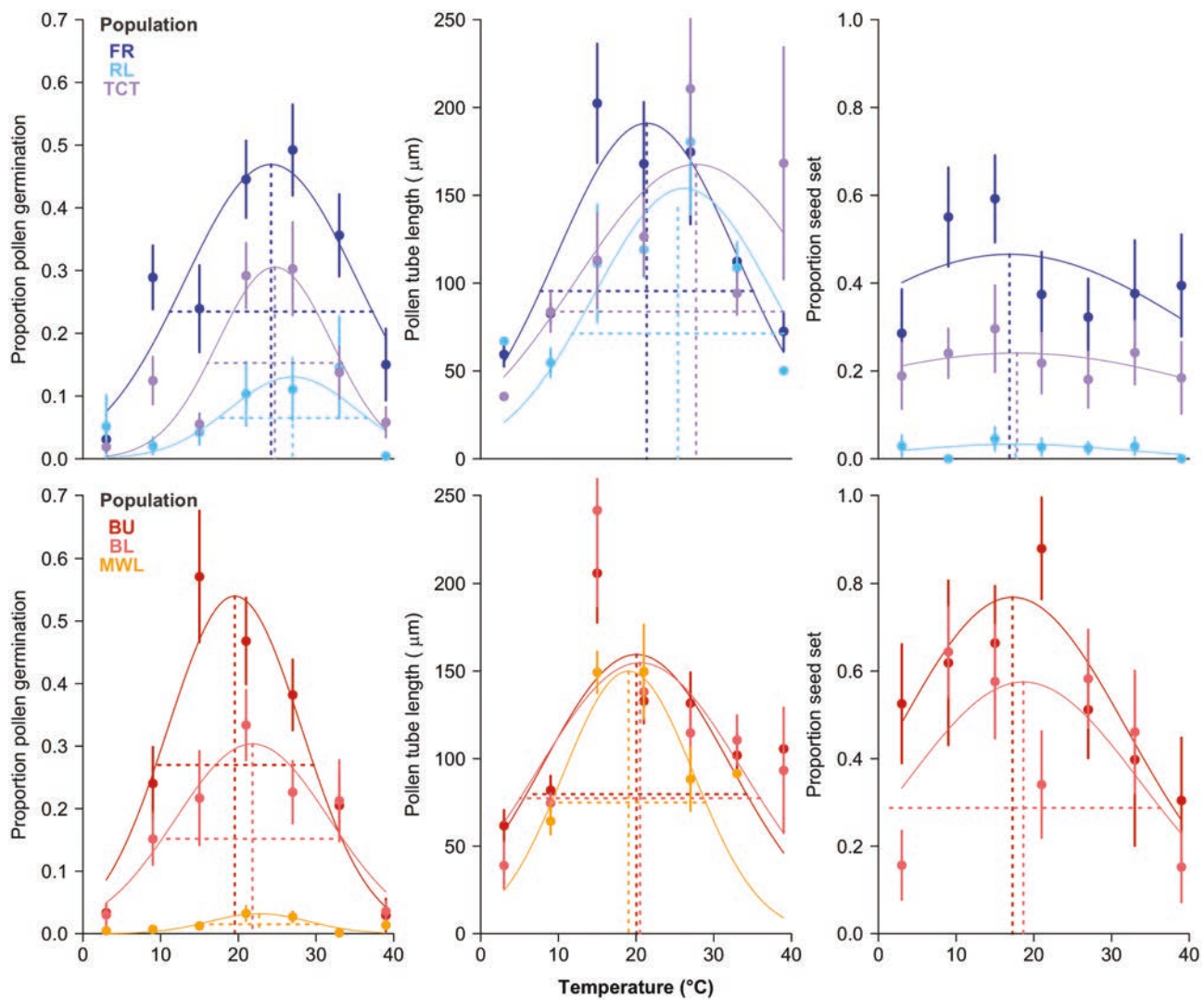


**Figure 3.** Gaussian thermal performance curves for pollen germination proportion, pollen tube length ( $\mu\text{m}$ ), and seed set in six populations of *Argentina anserina* from southwest Colorado. Optimal temperatures ( $T_{\text{opt}}$ ) and the width of the curve at 50% peak performance ( $B_{50}$ ) are provided if the standard deviation term from the fit is significant. Y-axes ranges differ among populations to highlight variation in  $T_{\text{opt}}$  and  $B_{50}$  among populations. The top row of panels represents high-elevation populations, while the bottom row represents low-elevation populations. Seed set is omitted for MWL because no flowers from this population set seed in any temperature treatment.

### Tolerance breadth

The distance between the thermal optimum and ambient temperatures did not predict  $B_{50}$  for any performance metric generated using Gaussian TPCs using long-term or flower-level ambient temperature (pollen germination: *long-term*  $T_4 = 0.17$ ,  $p = .87$ ,  $r = 0.08$ ; *flower-level*  $T_3 = -0.67$ ,  $p = .55$ ,  $r = -0.36$ . Pollen tube growth: *long-term*  $T_4 = 1.30$ ,  $p = 0.26$ ,  $r = 0.55$ ; *flower-level*  $T_3 = 1.28$ ,  $p = .29$ ,  $r = 0.6$ . Seed set: *long-term*  $T_3 = 1.00$ ,  $p = .39$ ,  $r = 0.50$ ; *flower-level*  $T_3 = 1.49$ ,  $p = .23$ ,  $r = 0.65$ ).

For pollen germination, TPCs modeled using the beta distribution, the degree of left-skewed asymmetry for  $B_{50}$  was positively associated with how high the optimum was above mean ambient temperatures (long-term ambient  $r = 0.89$ ,  $p = .017$ ; flower-level ambient,  $r = 0.94$ ,  $p = .014$ ; [Supplementary Figures S3 and S4](#)). That is, when optima far exceeded ambient temperatures, tolerance breadth was skewed towards ambient temperatures (see [Figure 1B](#)).

### Floral warming and cooling

Flowers warmed above ambient temperatures during the day but fell slightly below ambient temperatures at night ([Figure](#)

[4](#); [Supplementary Table S5A](#)). Flowers in high-elevation populations warmed significantly more above ambient than those in low ([Figure 4](#); [Supplementary Table S5A](#)). On average, high-elevation flowers were  $2.43^\circ\text{C}$  above ambient while low-elevation flowers were  $2.11^\circ\text{C}$  above ambient during mid-day (10:01–14:00, 15% difference [Figure 4](#); [Supplementary Table S5A](#)). During the afternoon (14:01–18:00), high-elevation flowers were  $1.1^\circ\text{C}$  warmer than ambient while low were  $0.72^\circ\text{C}$  above ambient (53% difference, [Figure 4](#); [Supplementary Table S5A](#)). There was no difference in  $\Delta T$  between elevations at any other time ([Figure 4](#)).

### Effect of the perianth on intrafloral temperature

Intrafloral temperatures were greater in flowers with intact perianths in low (mean  $\Delta T$ :  $3.07_{\text{intact}}$  vs.  $1.56_{\text{removed}}$ ) and high (mean  $\Delta T$ :  $3.16_{\text{intact}}$  vs.  $1.86_{\text{removed}}$ ) elevation populations from 10:01 to 14:00 ([Supplementary Table S5C](#)). This difference persisted between 14:01 and 18:00 in high-elevation populations (mean  $\Delta T$ :  $1.66_{\text{intact}}$  vs.  $0.87_{\text{removed}}$ ) but was absent in low elevations ([Figure 5](#); [Supplementary Table S5C](#)). Thus,

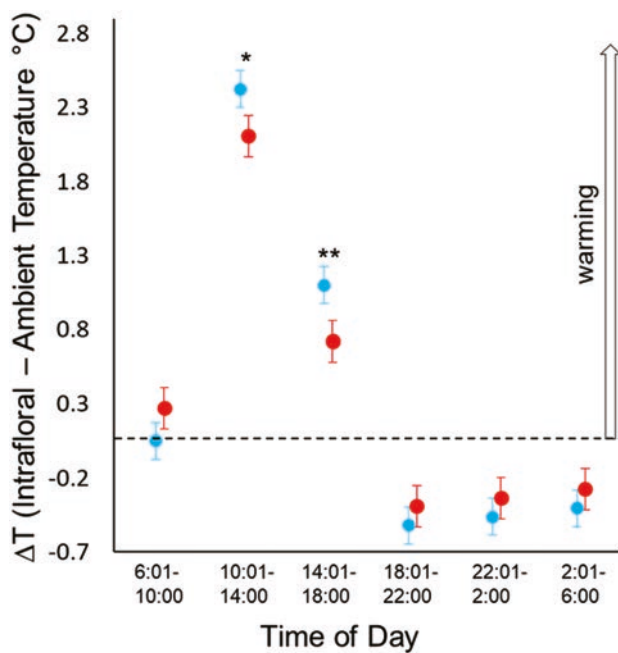


**Figure 4.** Difference between intrafloral and ambient temperature ( $\Delta T$ ) across 24-hr period for low and high elevation populations of *Argentina anserina*. Points depict estimated marginal means  $\pm 95\%$  CIs from a model accounting for population and flower identity. The dashed line indicates no difference between intrafloral and ambient temperatures. Asterisks denote significant differences between elevation clusters within time bins from post hoc Tukey tests,  $*p < .05$ ,  $**p < .01$ .

**Table 3.** Results of one-way Z-tests comparing optimal performance temperatures of pollen germination, pollen tube growth, and seed set to the minimum, mean, and maximum temperatures experienced by flowers in the field at three temporal and two spatial scales. Long-term: ambient temperature  $\sim 2$  m above soil surface during peak flowering (June–July, 1969–2020). 24-hr Intrafloral: temperature at the surface of the floral disc recorded over a 24-hr period in 2021. Daytime Intrafloral: Temperature at the surface of the floral disk from 10:00 to 18:00 h in 2021.

Scale	Elevation	Temperature 95% CI			Z	Pollen germination	Pollen tube growth	Seed set
		Min	Mean	Max				
Long-term	Low <i>n</i> = 3	Min	[2.99, 4.61]		-42.31	-38.72	-34.14	
		Mean	[13.19, 13.47]		-112.63	-91.70	-65.01	
		Max	[22.34, 23.41]		5.57	11.03	17.99	
	High <i>n</i> = 3	Min	[1.07, 1.38]		-312.15	-309.30	-207.56	
		Mean	[8.21, 9.32]		-58.62	-57.84	-30.03	
		Max	[15.05, 17.56]		-14.05	-13.71	-1.45	
24 hr Intrafloral	Low <i>n</i> = 5	Min	[2.07, 4.95]		-24.29	-22.27	-19.68	
		Mean	[14.69, 16.04]		-17.37	-13.05	-7.53	
		Max	[35.90, 37.07]		50.59	55.57	61.92	
	High <i>n</i> = 4	Min	[1.16, 2.52]		-67.42	-66.79	-44.23	
		Mean	[12.05, 14.07]		-23.88	-23.45	-8.14	
		Max	[32.93, 35.93]		11.93	12.22	22.48	
Daytime Intrafloral	Low <i>n</i> = 5	Min	[14.32, 16.45]		-11.00	-8.25	-4.75	
		Mean	[23.72, 24.75]		11.08	16.80	24.10	
		Max	[34.57, 35.32]		71.24	79.05	89.01	
	High <i>n</i> = 4	Min	[12.58, 17.66]		-7.86	-7.69	-1.63	
		Mean	[20.31, 24.66]		-2.54	-2.34	4.72	
		Max	[29.93, 34.61]		5.83	6.01	12.59	

Bold  $p < .01$ .

perianth tissue contributed to intrafloral warming and did so for a longer duration in high-elevation populations.

## Discussion

For species distributed across wide temperature gradients, populations at one extreme must cope with different thermal environments than those at the opposite extreme. Mobile organisms may rely, at least in part, on behavioral modification to meet the demands of disparate thermal environments (e.g., Huey, 1974; May, 1979; Terrien et al. 2011). Barring phenological escape (e.g., Rathcke & Lacey, 1985), sessile organisms must rely on (1) the evolution of thermal performance optima or tolerance to match local conditions (e.g., Buerger et al., 2020), or (2) physiological or morphological mechanisms mediating the effect of ambient temperature extremes (e.g., Knight & Ackerly, 2003; Kozlowski & Pallardy, 2002). We assessed three non-mutually exclusive scenarios of local adaptation to thermal environments (Figure 1) at the extremes of a 1000 m elevation gradient.

In the first scenario, thermal optima are shaped directly by the local thermal environment, resulting in thermal optima that closely match local thermal conditions during floral anthesis (Figure 1A). In *A. anserina*, gametic thermal optima largely fell between the ambient mean and maximum temperatures in low- and high-elevation populations (Figure 2A–F). One exception to this overall pattern was the high-elevation long-term ambient maxima, which was less than the high-elevation pollen optima (Figure 2A). However, this result

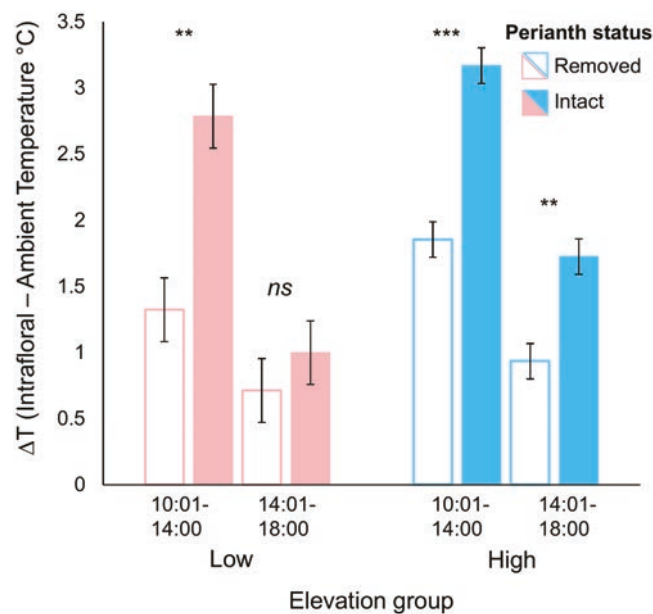


**Figure 5.** The effect of the perianth on heat accumulation of floral reproductive structures in low- and high-elevation populations of *A. anserina* between 12:00 and 16:00, and 16:01 and 20:00. Asterisks indicate significance between treated flowers (perianth removed) and control flowers (perianth intact) within an elevation cluster and time bin. \*\* $p < .01$ , \*\*\* $p < .0001$ . The overall effect of elevation  $\times$  floral treatment  $\times$  time bin effect on  $\Delta T$  was  $p < .0001$ .

may be explained by long-term estimates being derived from coarser-grained measurements (monthly means, 2 m above the soil surface, and at 4 km resolution) relative to flower-level measurements, and thus underestimating temperature extremes. This highlights the importance of measuring the operative thermal environment rather than solely relying on climate databases. Overall, the positioning of the gametic optima between thermal means and maximum is consistent with other studies showing that thermal performance curves may be shaped by both mean and extreme temperatures (Bennett et al., 2021; Ladinig et al., 2015).

Inconsistent with local adaptation of the gametic optima to divergent thermal environments, cooler high-elevation populations had greater gametic thermal performance optima than warmer low-elevation populations. While counterintuitive, greater thermal optima in high-elevation populations relative to low have been observed in other systems. Specifically, Higgins et al. (2014) describe a positive relationship between thermal optima for feeding and elevation in *Colias spp.* larvae which they attributed to a shorter growing season and warmer daily temperature variation at high elevations. However, as feeding involves fundamentally different processes from gamete performance, and high-elevation populations of *A. anserina* did not experience greater temperature variation than low, we must look elsewhere for answers to the question: *Why are gametic performance optima greater in populations that experience cooler ambient conditions in this system?*

First, selection on pollen thermal performance could occur outside of the floral environment. *Argentina anserina* is self-incompatible (Cisternas-Fuentes et al., 2022), and thus requires pollen transfer by bees and flies for sexual reproduction (Koski & Ashman, 2015). The bodies of insect pollinators

can dramatically exceed ambient temperatures, and heat accumulation is more pronounced in insects with larger body size (Bishop & Ambruster, 1999). Body size of both bees and flies at the community level has been shown to increase with elevation (McCabe et al., 2019). Furthermore, recent evidence suggests that thoracic heat accumulation may be particularly pronounced during pollen foraging with this effect increasing as the mass of the pollen load born by the forager increases (Naumchik & Youngsteadt, 2023). It is possible that selection on pollen thermal performance occurs during transfer on pollinators bodies, and that pollinator bodies may be warmer at high elevation than low. This may be the case if animals foraging on *A. anserina* at high elevation tend to be larger, produce more heat during flight, maintain larger pollen loads during a foraging bout, or forage during warmer times of day than at low elevation.

Second, genetic drift and isolation may provide explanations for population optima that do not conform to the local thermal environment. In *A. anserina*, there is phylogenomic evidence of serial migration from low- to high-elevation populations on the same gradient used in the present study (Cisternas-Fuentes & Koski, 2023), which is accompanied by reduced effective population size at high elevation. Serial colonization events toward range edges are often associated with accumulation of maladaptive alleles, termed the “expansion load” (Excoffier et al., 2009) which is consistent with the strong deviation of pollen thermal optima from ambient temperatures at high-elevation range limit. Moreover, high-elevation populations in this study are strongly isolated from both low-elevation populations, as well as one another (Cisternas-Fuentes & Koski, 2023). Limited gene flow into high-elevation populations could reduce the likelihood of local adaptation. Together, small effective population sizes and isolation may limit the capacity for high-elevation populations to respond to selection imposed by the thermal environment (Colautti & Lau, 2015; Hoffmann et al., 2017; Willi et al., 2006).

In the second scenario depicted in Figure 1B, thermal tolerance breadths increase as the distance between the environmental temperature and the gametic thermal optima increase. That is—this scenario represents an adaptive hypothesis under which a sub-optimal thermal environment selects for increased tolerance breadth. Based on the fact that high-elevation population optima for pollen deviated further from ambient temperatures, high-elevation populations should have wider tolerance breadths. We found no relationship between the distance of the optima from the environmental temperature (ambient means) and the thermal tolerance breadth (measured as  $B_{50}$ ) for any gametic performance metric. However, there was evidence that there was more asymmetry in tolerance breadth for pollen germination in high-elevation populations than low when modeled using a beta distribution. This result is consistent with the evolution of enhanced asymmetry in tolerance breadth in the direction of environmental temperatures. Thus, our results do not suggest local adaptation via overall expansion of thermal tolerance breadth, but some support for adaptation via stronger asymmetry in tolerance breadth when optima deviate far from environmental temperatures.

Finally, thermoregulatory mechanisms may help to achieve or maintain temperatures closer to performance optima (Figure 1C). In high-elevation populations, the presence of the perianth warmed flowers, bringing them closer to the thermal optima for pollen. At low elevation, perianth tissue

also warmed flowers, but did so to a lesser extent and over a shorter duration than high-elevation flowers. These results are consistent with selection favoring enhanced floral warming when gametic optima deviate more strongly above ambient temperatures, as depicted in **Figure 1C**. Despite this, pollen performance optima still exceeded the warming potential of high-elevation flowers, suggesting either constraints on floral heat accumulation or selection on pollen thermal optima outside of the floral environment.

In a number of species, petal orientation facilitates the accumulation of solar radiation, thereby raising intrafloral temperatures (Cooley, 1995; Patiño et al., 2002; Sapir et al., 2006). This can bring intrafloral temperatures closer to gametic thermal optima (McKee & Richards, 1998), as appears to be the case in high-elevation populations of *A. anserina*. Heat accumulation may however result in excess heat which appears to be the case in low-elevation populations where daytime floral temperatures exceed gametic optima. Increased floral heat accumulation in high-elevation populations compared to low could be conferred by a variety of factors such as elevational divergence in floral traits associated with heat capture or dissipation (e.g.: petal orientation, Kevan, 1975; floral evapotranspiration, Galen, 2006; Roddy, 2019), or more intense solar irradiance at high elevations (Dvorkin & Steinberger, 1999). While the mechanisms underlying differential floral warming across the elevation gradient are currently under investigation, the perianth removal study showed that the presence of petals and sepals increases the duration of floral warming in high-elevation populations relative to low. This suggests that elevational differences in flower morphology likely contribute to differential warming across the elevation gradient.

Regardless of enhanced floral warming at high elevation, high-elevation flowers were most often below optimal temperatures for pollen (**Supplementary Figure S2**). It is possible that the capacity for heat accumulation of the corolla is insufficient to achieve optimal intrafloral temperatures, especially given the counteracting effects of wind and cloud shadow. Alternatively, the thermal tolerances of petal tissue (e.g., Ladinig et al., 2015) or thermal preferences of pollinators (e.g., Corbet & Huang, 2016) may present conflicting selection pressures on floral heat accumulation capacity. Likewise, sexual conflict could explain why high-elevation populations do not warm flowers to the optima for pollen. For instance, at both low and high elevation, floral warming during the day exceeds the thermal optimum for ovule performance. A response to selection favoring floral warming may therefore be limited by costs of overheating ovules.

## Conclusions

Finding that gametic thermal optima are situated between mean and maximum intrafloral temperatures is generally consistent with balancing selection on the gametic thermal optima. However, as high-elevation pollen thermal optima were far above low-elevation pollen optima, elevational differences in ambient temperatures do not appear to fully explain the differences in optima between elevations. These results, paired with the result that corolla tissue warmed the intrafloral environment significantly more in high-elevation populations than low, points to regulation of the floral environment as a target of selection across the gradient. Indeed, stronger floral warming at high elevation brings pollen closer

to its thermal optimum, while reduced floral warming in low elevation should limit overheating of pollen and ovules. While we found no support for local adaptation of gametic thermal optima (**Figure 1A**) there was limited support for local adaptation of the shape of thermal tolerance breadth (**Figure 1B**), and suggestion that elevational divergence in floral warming may be a response to the thermal demands of pollen and ovules (**Figure 1C**). In our effort to understand intraspecific variation of the abiotic optima of gametophytes housed within flowers, this work highlights the interplay between ecophysiology and geographic variation in shaping plant reproductive ecology and floral evolution.

## Supplementary material

Supplementary material is available online at *Evolution*.

## Data availability

All data associated with this manuscript are archived with Open Science Framework DOI: 10.17605/OSF.IO/UBFZW

## Author contributions

M.K. conceived of and M.K. and J.H. designed the study; M.K. and J.H. performed field and lab work, and conducted statistical analyses. J.H. led the writing with input from M.K. Both authors contributed to the conceptual development and edited the text.

## Funding

This work was funded by the National Science Foundation (DEB-2015459) to M.K. Any opinions, findings, and conclusions or recommendations expressed in this material are those of the authors and do not necessarily reflect the views of the National Science Foundation.

*Conflict of interest:* The authors declare no conflict of interest.

## Acknowledgments

The authors thank L. Finnell and A. Cisternas Fuentes for field and greenhouse assistance; G. Calabrese for programming advice; W. Witman, C. Gaskins, and T. Sherer for lab assistance, as well as J. Friedman and three anonymous reviewers for valuable feedback on the initial manuscript.

## References

- Angilletta, M. J. (2006). Estimating and comparing thermal performance curves. *Journal of Thermal Biology*, 31(7), 541–545. <https://doi.org/10.1016/j.jtherbio.2006.06.002>
- Bates, D., Maechler, M., Bolker, B., & Walker, S. (2015). Fitting linear mixed-effects models using lme4. *Journal of Statistical Software*, 67(1), 1–48. <https://doi.org/10.18637/jss.v067.i01>
- Bennett, A. C., Arndt, S. K., Bennett, L. T., Knauer, J., Beringer, J., Griebel, A., Hinko-Najera, N., Liddell, M. J., Metzen, D., Pendall, E., Silberstein, R. P., Wardlaw, T. J., Woodgate, W., & Haverd, V. (2021). Thermal optima of gross primary productivity are closely aligned with mean air temperatures across Australian woodland ecosystems. *Global Change Biology*, 27(19), 4727–4744. <https://doi.org/10.1111/gcb.15760>

Bishop, J. A., & Armbruster, W. S. (1999). Thermoregulatory abilities of Alaskan bees: Effects of size, phylogeny and ecology. *Functional Ecology*, 13(5), 711–724. <https://doi.org/10.1046/j.1365-2435.1999.00351.x>

Buckley, L. B., Ehrenberger, J. C., & Angilletta, M. J. (2015). Thermoregulatory behaviour limits local adaptation of thermal niches and confers sensitivity to climate change. *Functional Ecology*, 29(8), 1038–1047. <https://doi.org/10.1111/1365-2435.12406>

Buerger, P., Alvarez-Roa, C., Coppin, C. W., Pearce, S. L., Chakravarti, L. J., Oakeshott, J. G., Edwards, O. R., & Van Oppen, M. J. H. (2020). Heat-evolved microalgal symbionts increase coral bleaching tolerance. *Science Advances*, 6(20), eaba2498. <https://doi.org/10.1126/sciadv.aba2498>

Chaturvedi, P., Wiese, A. J., Ghatak, A., Zaveska Drabkova, L., Weckwerth, W., & Honys, D. (2021). Heat stress response mechanisms in pollen development. *The New Phytologist*, 231(2), 571–585. <https://doi.org/10.1111/nph.17380>

Cisternas-Fuentes, A., Dwyer, R., Johnson, N., Finnell, L., Gilman, J., & Koski, M. H. (2022). Disentangling the components of pollen limitation in a widespread herb with gametophytic self-incompatibility. *American Journal of Botany*, 110(2), e16122. <https://doi.org/10.1002/ajb2.16122>

Cisternas-Fuentes, A., & Koski, M. H. (2023). Drivers of strong isolation and small effective population size at a leading range edge of a widespread plant. *Heredity*, 130(6), 347–357. <https://doi.org/10.1038/s41437-023-00610-z>

Clay, T. A., & Gifford, M. E. (2017). Population level differences in thermal sensitivity of energy assimilation in terrestrial salamanders. *Journal of Thermal Biology*, 64, 1–6. <https://doi.org/10.1016/j.jthbir.2016.12.006>

Clench, H. K. (1966). Behavioral thermoregulation in butterflies. *Ecology*, 47(6), 1021–1034. <https://doi.org/10.2307/1935649>

Chirgwin, E., Connallon, T., & Monro, K. (2021). The thermal environment at fertilization mediates adaptive potential in the sea. *Evolution Letters*, 5(2), 154–163. <https://doi.org/10.1002/evl3.215>

Colautti, R. I., & Lau, J. A. (2015). Contemporary evolution during invasion: Evidence for differentiation, natural selection, and local adaptation. *Molecular Ecology*, 24(9), 1999–2017. <https://doi.org/10.1111/mec.13162>

Cooley, J. R. (1995). Floral heat rewards and direct benefits to insect pollinators. *Annals of the Entomological Society of America*, 88(4), 576–579. <https://doi.org/10.1093/esa/88.4.576>

Corbet, S. A., & Huang, S. Q. (2016). Small bees overheat in sunlit flowers: Do they make cooling flights? *Ecological Entomology*, 41(3), 344–350. <https://doi.org/10.1111/een.12307>

Corbett, A. L., Krannitz, P. G., & Aarsen, L. W. (1992). The influence of petals on reproductive success in the arctic poppy (*Papaver radicatum*). *Canadian Journal of Botany*, 70(1), 200–204.

Creux, N. M., Brown, E. A., Garner, A. G., Saeed, S., Scher, C. L., Holalu, S. V., Yang, D., Maloof, J. N., Blackman, B. K. & Harmer, S. L. (2021). Flower orientation influences floral temperature, pollinator visits and plant fitness. *New Phytologist*, 232(2), 868–879.

Davies, P. L., & Hew, C. L. (1990). Biochemistry of fish antifreeze proteins. *FASEB Journal*, 4(8), 2460–2468. <https://doi.org/10.1096/fasebj.4.8.2185972>

Dvorkin, A. Y., & Steinberger, E. H. (1999). Modeling the altitude effect on solar UV radiation. *Solar Energy*, 65(3), 181–187. [https://doi.org/10.1016/s0038-092x\(98\)00126-1](https://doi.org/10.1016/s0038-092x(98)00126-1)

Elzhov, T. V., Mullen, K. M., Spiess, A. N., Bolker, B., Mullen, M. K. M., & Suggests, M. A. S. S. (2016). Package “minpack.lm.” R Interface Levenberg-Marquardt Nonlinear Least-Sq. Algorithm Found MINPACK Plus Support Bounds. <https://cran.r-project.org/web/packages/minpack.lm/minpack.lm.pdf>

Excoffier, L., Foll, M., & Petit, R. J. (2009). Genetic consequences of range expansions. *Annual Review of Ecology, Evolution, and Systematics*, 40(1), 481–501. <https://doi.org/10.1146/annurev.ecolsys.39.110707.173414>

Flores-Rentería, L., Whipple, A. V., Benally, G. J., Patterson, A., Canyon, B., & Gehring, C. A. (2018). Higher temperature at lower elevation sites fails to promote acclimation or adaptation to heat stress during pollen germination. *Frontiers in Plant Science*, 9, 536. <https://doi.org/10.3389/fpls.2018.00536>

Galen, C. (2006). Solar furnaces or swamp coolers: Costs and benefits of water use by solar-tracking flowers of the alpine snow buttercup, *Ranunculus adoneus*. *Oecologia*, 148(2), 195–201. <https://doi.org/10.1007/s00442-006-0362-y>

Galen, C., & Stanton, M. L. (2003). Sunny-side up: Flower heliotropism as a source of parental environmental effects on pollen quality and performance in the snow buttercup, *Ranunculus adoneus* (Ranunculaceae). *American Journal of Botany*, 90(5), 724–729.

Gaston, K. J., Chown, S. L., Calosi, P., Bernardo, J., Bilton, D. T., Clarke, A., Clusella-Trullas, S., Ghalambor, C. K., Konarzewski, M., Peck, L. S., Porter, W. P., Pörtner, H. O., Rezende, E. L., Schulte, P. M., Spicer, J. I., Stillman, J. H., Terblanche, J. S., & van Kleunen, M. (2009). Macrophysiology: A conceptual reunification. *The American Naturalist*, 174(5), 595–612. <https://doi.org/10.1086/605982>

Gates, D. M. (1968). Transpiration and leaf temperature. *Annual Review of Plant Physiology*, 19(1), 211–238. <https://doi.org/10.1146/annurev.pp.19.060168.001235>

Geange, S. R., Arnold, P. A., Catling, A. A., Coast, O., Cook, A. M., Gowland, K. M., Leigh, A., Notarnicola, R. F., Posch, B. C., Venn, S. E., Zhu, L., & Nicotra, A. B. (2021). The thermal tolerance of photosynthetic tissues: A global systematic review and agenda for future research. *The New Phytologist*, 229(5), 2497–2513. <https://doi.org/10.1111/nph.17052>

Gezon, Z. J., Inouye, D. W., & Irwin, R. E. (2016). Phenological change in a spring ephemeral: Implications for pollination and plant reproduction. *Global Change Biology*, 22(5), 1779–1793. <https://doi.org/10.1111/gcb.13209>

Gilbert, A. L., & Miles, D. B. (2019). Spatiotemporal variation in thermal niches suggests lability rather than conservatism of thermal physiology along an environmental gradient. *Biological Journal of the Linnean Society*, 128(2), 263–277. <https://doi.org/10.1093/biolin/blz093>

Giorno, F., Wolters-Arts, M., Mariani, C., & Rieu, I. (2013). Ensuring reproduction at high temperatures: The heat stress response during anther and pollen development. *Plants (Basel, Switzerland)*, 2(3), 489–506. <https://doi.org/10.3390/plants2030489>

Griffith, M., & Yaish, M. W. F. (2004). Antifreeze proteins in overwintering plants: A tale of two activities. *Trends in Plant Science*, 9(8), 399–405. <https://doi.org/10.1016/j.tplants.2004.06.007>

Harrap, M. J., Rands, S. A., Hempel de Ibarra, N., & Whitney, H. M. (2017). The diversity of floral temperature patterns, and their use by pollinators. *Elife*, 6, e31262.

Hatfield, J. L., & Prueger, J. H. (2015). Temperature extremes: Effect on plant growth and development. *Weather and Climate Extremes*, 10, 4–10. <https://doi.org/10.1016/j.wace.2015.08.001>

Heinrich, B., & Esch, H. (1994). Thermoregulation in bees. *American Scientist*, 82(2), 164–170.

Higgins, J. K., MacLean, H. J., Buckley, L. B., & Kingsolver, J. G. (2014). Geographic differences and microevolutionary changes in thermal sensitivity of butterfly larvae in response to climate. *Functional Ecology*, 28(4), 982–989. <https://doi.org/10.1111/1365-2435.12218>

Hoffmann, A. A., Sgrò, C. M., & Kristensen, T. N. (2017). Revisiting adaptive potential, population size, and conservation. *Trends in Ecology & Evolution*, 32(7), 506–517. <https://doi.org/10.1016/j.tree.2017.03.012>

Huey, R. B. (1974). Behavioral thermoregulation in lizards: Importance of associated costs. *Science*, 184(4140), 1001–1003. <https://doi.org/10.1126/science.184.4140.1001>

Huey, R. B., & Stevenson, R. D. (1979). Integrating thermal physiology and ecology of ectotherms: A discussion of approaches. *American Zoologist*, 19(1), 357–366.

Janzen, D. H. (1967). Why mountain passes are higher in the tropics. *The American Naturalist*, 101(919), 233–249. <https://doi.org/10.1086/282487>

Kearns, C. A., & Inouye, D. W. (1993). *Techniques for pollination biologists*. University Press of Colorado.

Kevan, P. G. (1972). Heliotropism in some arctic flowers. *The Canadian Field Naturalist*, 86, 41–44.

Kevan, P. G. (1975). Sun-tracking solar furnaces in high arctic flowers: Significance for pollination and insects. *Science*, 189(4204), 723–726.

Kingsolver, J. G. (1987). Evolution and coadaptation of thermoregulatory behavior and wing pigmentation pattern in Pierid butterflies. *Evolution*, 41(3), 472–490. <https://doi.org/10.1111/j.1558-5646.1987.tb05819.x>

Kingsolver, J. G., & Woods, H. A. (2016). Beyond thermal performance curves: Modeling time-dependent effects of thermal stress on ectotherm growth rates. *The American Naturalist*, 187(3), 283–294. <https://doi.org/10.1086/684786>

Knight, C. A., & Ackery, D. D. (2003). Evolution and plasticity of photosynthetic thermal tolerance, specific leaf area and leaf size: Congeneric species from desert and coastal environments. *The New Phytologist*, 160(2), 337–347. <https://doi.org/10.1046/j.1469-8137.2003.00880.x>

Kooi, C. J. van der, Kevan, P. G., & Koski, M. H. (2019). The thermal ecology of flowers. *Annals of Botany*, 124(3), 343–353. <https://doi.org/10.1093/aob/mcz073>

Koski, M. H., & Ashman, T. -L. (2015). An altitudinal cline in UV floral pattern corresponds with a behavioral change of a generalist pollinator assemblage. *Ecology*, 96(12), 3343–3353. <https://doi.org/10.1890/15-0242.1>

Koski, M. H., Finnell, L. M., Leonard, E., & Tharayil, N. (2022). Elevational divergence in pigmentation plasticity is associated with selection and pigment biochemistry. *Evolution*, 76(3), 512–527.

Kozlowski, T. T., & Pallardy, S. G. (2002). Acclimation and adaptive responses of woody plants to environmental stresses. *The Botanical Review*, 68(2), 270–334. [https://doi.org/10.1663/0006-8101\(2002\)068\[0270:aaarow\]2.0.co;2](https://doi.org/10.1663/0006-8101(2002)068[0270:aaarow]2.0.co;2)

Lacey, E. P., Lovin, M. E., Richter, S. J., & Herington, D. A. (2010). Floral reflectance, color, and thermoregulation: What really explains geographic variation in thermal acclimation ability of ectotherms? *The American Naturalist*, 175(3), 335–349. <https://doi.org/10.1086/650442>

Laloi, M., Klein, M., Riesmeier, J. W., Müller-Röber, B., Fleury, C., Bouillaud, F., & Ricquier, D. (1997). A plant cold-induced uncoupling protein. *Nature*, 389(6647), 135–136. <https://doi.org/10.1038/38156>

Ladinig, U., Pramsohler, M., Bauer, I., Zimmermann, S., Neuner, G., & Wagner, J. (2015). Is sexual reproduction of high-mountain plants endangered by heat? *Oecologia*, 177(4), 1195–1210. <https://doi.org/10.1007/s00442-015-3247-0>

Leith, N. T., Fowler-Finn, K. D., & Moore, M. P. (2022). Evolutionary interactions between thermal ecology and sexual selection. *Ecology Letters*, 25(9), 1919–1936.

Lenth, R. (2022). *emmeans: Estimated marginal means, aka least-squares means\_. R package version 1.8.3*. <https://CRAN.R-project.org/package=emmeans>

May, M. L. (1979). Insect thermoregulation. *Annual Review of Entomology*, 24(1), 313–349. <https://doi.org/10.1146/annurev.en.24.010179.001525>

Marer, L., & Cai, G. (2022). Pollen priming for more efficient reproduction in a heating world: What we know, what we need to know. *Plant Stress*, 3, 100060. <https://doi.org/10.1016/j.plstress.2022.100060>

McCabe, L. M., Colella, E., Chesshire, P., Smith, D., & Cobb, N. S. (2019). The transition from bee-to-fly dominated communities with increasing elevation and greater forest canopy cover. *PLoS One*, 14(6), e0217198–e0217198. <https://doi.org/10.1371/journal.pone.0217198>

McKee, J., & Richards, A. J. (1998). Effect of flower structure and flower colour on intrafloral warming and pollen germination and pollen-tube growth in winter flowering Crocus L(Iridaceae). *Botanical Journal of the Linnean Society*, 128(4), 369–384. <https://doi.org/10.1111/j.1095-8339.1998.tb02127.x>

National Oceanic and Atmospheric Administration. (2018). *Comparative climatic data*. National Centers for Environmental Information. <https://www1.ncdc.noaa.gov/pub/data/ccd-data/relhum18.dat>

Naumchik, M., & Youngsteadt, E. (2023). Larger pollen loads increase risk of heat stress in foraging bumblebees. *Biology Letters*, 19(5), 20220581. <https://doi.org/10.1098/rsbl.2022.0581>

Navas, C. A. (1997). Thermal extremes at high elevations in the Andes: Physiological ecology of frogs. *Journal of Thermal Biology*, 22(6), 467–477. [https://doi.org/10.1016/s0306-4565\(97\)00065-x](https://doi.org/10.1016/s0306-4565(97)00065-x)

Palaima, A., & Spitzke, K. (2004). Is a jack-of-all-temperatures a master of none? An experimental test with *Daphnia pulicaria* (Crustacea: Cladocera). *Evolutionary Ecology Research*, 6(2), 215–225.

Patiño, S., & Grace, J. (2002). The cooling of convolvulaceous flowers in a tropical environment. *Plant, Cell & Environment*, 25(1), 41–51.

Patiño, S., Jeffree, C., & Grace, J. (2002). The ecological role of orientation in tropical Convolvulaceous flowers. *Oecologia*, 130(3), 373–379. <https://doi.org/10.1007/s00442-001-0824-1>

Pither, J. (2003). Climate tolerance and interspecific variation in geographic range size. *Proceedings of the Royal Society B: Biological Sciences*, 270(1514), 475–481. <https://doi.org/10.1098/rspb.2002.2275>

Porcelli, D., Gaston, K. J., Butlin, R. K., & Snook, R. R. (2017). Local adaptation of reproductive performance during thermal stress. *Journal of Evolutionary Biology*, 30(2), 422–429. <https://doi.org/10.1111/jeb.13018>

PRISM Climate Group, Oregon State University. <https://prism.oregonstate.edu> (accessed September 1, 2021).

R Core Team. (2021). *R: A language and environment for statistical computing*. R Foundation for Statistical Computing. <https://www.R-project.org/>

Rathcke, B., & Lacey, E. P. (1985). Phenological patterns of terrestrial plants. *Annual Review of Ecology and Systematics*, 16(1), 179–214. <https://doi.org/10.1146/annurev.es.16.110185.001143>

Roddy, A. (2019). Energy balance implications of floral traits involved in pollinator attraction and water balance. *International Journal of Plant Sciences*, 180, 944–953.

Rosbakh, S., Pacini, E., Nepi, M., & Poschlod, P. (2018). An unexplored side of regeneration niche: Seed quantity and quality are determined by the effect of temperature on pollen performance. *Frontiers in Plant Science*, 9, 1036. <https://doi.org/10.3389/fpls.2018.01036>

Rosbakh, S., & Poschlod, P. (2016). Minimal temperature of pollen germination controls species distribution along a temperature gradient. *Annals of Botany*, 117(7), 1111–1120. <https://doi.org/10.1093/aob/mcw041>

Rousi, A. (1965). Biosystematic studies on the species aggregate *Potentilla anserina* L. *Annales Botanici Fennici*, 1, 47–112.

Sage, R. F., & Kubien, D. S. (2007). The temperature response of C3 and C4 photosynthesis. *Plant, Cell & Environment*, 30(9), 1086–1106. <https://doi.org/10.1111/j.1365-3040.2007.01682.x>

Sapir, Y., Shmida, A., & Ne'eman, G. (2006). Morning floral heat as a reward to the pollinators of the *Oncocyclops* irises. *Oecologia*, 147(1), 53–59. <https://doi.org/10.1007/s00442-005-0246-6>

Schlesinger, M. J. (1990). Heat shock proteins. *The Journal of Biological Chemistry*, 265(21), 12111–12114.

Schneider, C. A., Rasband, W. S., & Eliceiri, K. W. (2012). NIH image to ImageJ: 25 Years of image analysis. *Nature Methods*, 9(7), 671–675. <https://doi.org/10.1038/nmeth.2089>

Seebacher, F., & Franklin, C. E. (2005). Physiological mechanisms of thermoregulation in reptiles: A review. *Journal of Comparative Physiology B Biochemical Systemic and Environmental Physiology*, 175(8), 533–541. <https://doi.org/10.1007/s00360-005-0007-1>

Sheth, S. N., & Angert, A. L. (2014). The evolution of environmental tolerance and range size: A comparison of geographically restricted and widespread *Mimulus*. *Evolution*, 68(10), 2917–2931. <https://doi.org/10.1111/evol.12494>

Sinclair, B. J., Marshall, K. E., Sewell, M. A., Levesque, D. L., Willett, C. S., Slotsbo, S., Dong, Y., Harley, C. D., Marshall, D. J., Helmuth, B. S. & Huey, R. B. (2016). Can we predict ectotherm responses to climate change using thermal performance curves and body temperatures? *Ecology Letters*, 19(11), 1372–1385.

Smith, N. G., & Dukes, J. S. (2013). Plant respiration and photosynthesis in global-scale models: Incorporating acclimation to temperature and CO<sub>2</sub>. *Global Change Biology*, 19(1), 45–63. <https://doi.org/10.1111/j.1365-2486.2012.02797.x>

Stevens, G. C. (1989). The latitudinal gradient in geographical range: How so many species coexist in the tropics. *The American Naturalist*, 133(2), 240–256. <https://doi.org/10.1086/284913>

Sunday, J., Bennett, J. M., Calosi, P., Clusella-Trullas, S., Gravel, S., Hargreaves, A. L., Leiva, F. P., Verberk, W., Olalla-Tárraga, M. A., & Morales-Castilla, I. (2019). Thermal tolerance patterns across latitude and elevation. *Philosophical Transactions of the Royal Society B: Biological Sciences*, 374(1778), 20190036. <https://doi.org/10.1098/rstb.2019.0036>

Sunday, J. M., Bates, A. E., Kearney, M. R., Colwell, R. K., Dulvy, N. K., Longino, J. T., & Huey, R. B. (2014). Thermal-safety margins and the necessity of thermoregulatory behavior across latitude and elevation. *Proceedings of the National Academy of Sciences of the United States of America*, 111(15), 5610–5615. <https://doi.org/10.1073/pnas.1316145111>

Terrien, J., Perret, M., & Aujard, F. (2011). Behavioral thermoregulation in mammals: A review. *Frontiers in Bioscience-Landmark*, 16(4), 1428–1444.

Weber, W.A., & Wittman, R. C. (1996). *Colorado flora: Western slope*. Colorado Associated University Press.

Willi, Y., van Buskirk, J., & Hoffmann, A. A. (2006). Limits to the adaptive potential of small populations. *Annual Review of Ecology, Evolution, and Systematics*, 37(1), 433–458. <https://doi.org/10.1146/annurev.ecolsys.37.091305.110145>. <http://www.jstor.org/stable/30033839>

Yamori, W., Hikosaka, K., & Way, D. A. (2014). Temperature response of photosynthesis in C 3, C 4, and CAM plants: Temperature acclimation and temperature adaptation. *Photosynthesis Research*, 119(1-2), 101–117. <https://doi.org/10.1007/s11120-013-9874-6>

Zinn, K. E., Tunc-Ozdemir, M., & Harper, J. F. (2010). Temperature stress and plant sexual reproduction: Uncovering the weakest links. *Journal of Experimental Botany*, 61(7), 1959–1968. <https://doi.org/10.1093/jxb/erq053>